Published in final edited form as:
Mol Pharm. 2013 May 6; 10(5): 1910–1917. doi:10.1021/mp3006903.

pH-Sensitive Fluorescent Dyes: Are They Really pH-Sensitive in Cells?

Xiao-Xiang Zhang[1,‡], **Zhe Wang**[1,2,‡], **Xuyi Yue**[1,2], **Ying Ma**[1], **Dale O. Kiesewetter**[1], and **Xiaoyuan Chen**[1,*]

[1]Laboratory of Molecular Imaging and Nanomedicine (LOMIN), National Institute of Biomedical Imaging and Bioengineering (NIBIB), National Institutes of Health, Bethesda, Maryland 20892, USA

[2]Center for Molecular Imaging and Translational Medicine, School of Public Health, Xiamen University, Xiamen 361005, China

Abstract

Chemically synthesized near-infrared (NIR) aza-BODIPY dyes displayed OFF/ON fluorescence at acidic pH (pK_a = 6.2-6.6) through the suppression of photoinduced electron transfer (PET) and/or internal charge transfer (ICT) process. The apparent pK_as of the dyes were shifted well above physiological pH in hydrophobic microenvironment, which led to "turned-on" fluorescence in micelles and liposomes at neutral and basic pH. Bovine serum albumin (BSA) also activated the fluorescence, though to a much less extent. When these small molecular dyes entered cells, instead of being fluorescent only in acidic organelles, the whole cytoplasm exhibited fluorescence, with signal/background ratio as high as ~10 in no-wash live cell imaging. The dye **1** labeled cells remained highly fluorescent even after 3 days. Moreover, slight variations of the dye structure resulted in significantly different intracellular fluorescence behaviors, possibly due to their different cellular uptake and intracellular activation capabilities. After separation of cellular components, the fraction of plasma membrane and endoplasmic reticulum (ER) showed the highest fluorescence, further confirming the fluorescence activation by membrane structures. The fluorescence intensity of these dyes at different intracellular pH (6.80 and 8.00) did not differ significantly, indicating that intracellular pH did not play a critical role. Altogether, we showed here for the first time that the fluorescence of pH-sensitive aza-BODIPY dyes were switched intracellularly not by acidic pH, but by intracellular membranes (and proteins as well). The excellent membrane permeability, ultra high fluorescence contrast ratio, persistent fluorescent signal, and minimum biological interference of dye **1** make it an ideal choice for live cell imaging and *in vivo* cell tracking. These findings also imply that the intracellular fluorescent properties of pH-sensitive dyes should be carefully examined before used as pH indicators.

Keywords

aza-BODIPY; pH sensitive; pK_a change in membrane; fluorescent imaging

*Corresponding Author: shawn.chen@nih.gov.
‡**Author Contributions**: These authors contributed equally.

Supporting Information. Materials and instruments, synthetic details, fluorescence increase of dye **1** at different surfactant concentrations, fluorescence spectra of dyes **1**-**4** in micelles and liposomes, size of liposomes at different pH, confocal images of cells loaded with dyes **1**-**4** in the absence of serum, and the ROIs at different intracellular pH presented. This information is available free of charge via the internet at http://pubs.acs.org.

Introduction

Intracellular pH plays many critical roles in cell activities, such as proliferation and apoptosis,[1-3] ion transport,[4-6] multidrug resistance (MDR),[7] and endocytosis.[8] Abnormal intracellular pH values are associated with many diseases such as cancer[9] and Alzheimer's.[10] Inside the cells, low intracompartmental pH functions to denature proteins or to activate enzymes that are normally inactive around neutral pH. For instance, the acidic environment in lysosomes (pH 4.5-5.5)[11] can facilitate the degradation of proteins in cellular metabolism. The tightly regulated intracellular pH means that the precise measurement of intracellular pH can provide critical information on cellular functions and pathological processes. Compared with other pH measurement methods, such as microelectrodes, nuclear magnetic resonance (NMR), and absorbance spectroscopy, fluorescence spectroscopy has many advantages, including high sensitivity, high spatial and temporal resolution, operational simplicity, and, in most cases, is non-destructive to the cells.

The need of pH sensing has resulted in the development of many pH sensitive fluorescent probes; and they have been extensively reviewed by Han and Burgess recently.[12] Generally speaking, there are two types of pH sensitive fluorescent probes. The first type responds to pH changes around their pK_as with sharply changed fluorescence intensity, i.e. the “on-off” or “off-on” probes. The others are called ratiometric probes, which are differentially sensitive to pH at two excitation or emission wavelengths. However, many of them suffer from various drawbacks, such as photobleaching, small spectroscopic change upon pH change, sub-optimal Ex/Em wavelength, leakage from cells, and low absorbance or quantum yield under certain conditions. Therefore, better or optimal intracellular pH indicators are still needed.

The family of aza-BODIPY dyes has shown many advantages as fluorescent probes, such as high extinction coefficient, high quantum yield, long Ex/Em wavelength, insensitivity to solvents, and easy tunability through peripheral functionalization. Indeed, aza-BODIPY dyes have been used in fluorescence imaging,[13, 14] photodynamic therapy[15-17] and chemical sensing.[18-20] In this manuscript, we reported for the first time the intracellular fluorescence behavior of a series of pH-sensitive near-infrared (NIR) aza-BODIPY dyes (Scheme 1). The tertiary amines and/or phenols of these dye molecules have pK_as below 7. Their fluorescence can be “turned on” once the N- and/or O- are protonated at acidic pH through the efficient suppression of PET[15] (photoinduced electron transfer) and/or ICT[14] (internal charge transfer) process. These dyes are expected to show “switched-on” fluorescence responding to acidic intracellular pH. However, it is found that once inside the cells, the fluorescence of these dyes was “turned on”, not by bulk solution pH, but through the pK_a shift when incorporated in membranes and proteins. Among them, dye **1** showed excellent membrane permeability, ultra high fluorescence contrast ratio without washing the cells, prolonged fluorescence, and minimum biological interference, which make it an excellent choice for live cell imaging and *in vivo* cell tracking.

Experimental Section

Synthesis

The aza-BODIPY dyes were synthesized according to reported methods with some modifications.[17, 21] The synthetic route can be found in Scheme 1 and details can be found in the Supporting Information. Briefly, aldo condensation between aldehyde **6** and hydroxy- or methoxy- acetophenone, followed by a Michael addition reaction with nitromethane, afforded **8** or **11**. The azadipyrromethene structures were then synthesized in the presence of ammonium acetate. After the BF_2 complexes **1** or **2** were formed, reaction with methyl iodide gave the methylation products **3** or **4**

Fluorescence Response to pH in Bulk Solution, Micelles and Liposomes

Stock solutions of the dyes were prepared in DMSO. Na_2HPO_4/citric acid buffer was prepared using 0.1 M Na_2HPO_4 and 0.2 M citric acid, then adjusted to appropriate pH using 5 M NaOH or HCl. Micelle solutions were prepared in pH 7.40 PBS. To prepare liposomes, lecithin and cholesterol (85:15 w/w) were dissolved in chloroform and the solvent was removed under reduced pressure to form a thin layer. After further drying under vacuum overnight, liposomes were formed by rehydration using PBS of appropriate pH and subsequent bath sonication under N_2 at RT for 20 min. The final concentration of the liposomes was 1 mg/mL. The sizes of liposomes were measured by dynamic light scattering. In all the fluorescence measurements, the dye in DMSO (final DMSO 1.6% v/v) was added to the respective solution and incubated for 10 min at RT before measurement. For the fluorescence in micelles and liposomes, the results were normalized to FL = 100 under acidic conditions when maximal emission was achieved for each dye.

No-wash Live Cell Imaging

The day before imaging, MDA-MB-435 cells were plated on 8-well chambered glass slides or 35-mm glass bottom dishes. The cells reached 40-50% confluency at the time of imaging. Dyes in DMSO were added to cell media (final concentration: dye 0.1 μM, DMSO 0.5% v/v), and confocal images were taken directly at indicated time points. The dyes were excited at 635 nm using the same filter set employed for Cy5.5. The following microscopic settings were kept the same in all imaging experiments: laser intensity, 10%; sensitivity, 45%; and scan speed, 0.3 μs/pixel. Best effort was made to focus on the cytoplasm plane at each time point, albeit not all cells would be on the same focal plane. To calculate the intracellular/extracellular signal contrast ratios, intracellular regions of interest (ROIs) were chosen in cytoplasm areas; nuclei and plasma membranes were excluded.

For imaging at later time points, cells were incubated with dye **1** for 3 h. After the removal of media, the cells were washed with PBS (×3) and incubated with fresh growth media. Confocal images were taken at indicated time points.

Fluorescence Distribution in Cellular Fractions

Two days before experiment, cells were plated on 10 cm dishes. When the cells reached 50-60% confluency, dyes in DMSO were added (final concentration: dye 0.2 μM, DMSO 1% v/v). After incubating for 2 h, the medium was removed and cells were washed with PBS (×3) before being harvested by scraping at 4 °C. The obtained cell pellet was re-suspended in 200 μL PBS and lysed using probe sonication with 5 second pulse 3 times. The cellular components were then separated by differential centrifugation at 4 °C.[22] The pellet of each fraction was re-suspended in 200 μL PBS. Fluorescence was measured and normalized to % of total cellular fluorescence for each dye.

Adjustment of Intracellular pH

The method was adapted from literature report.[23] Cells were first incubated with dye **1** for 1 h. After removal of the dye and washing with K^+-rich buffer (130 mM KCl, 20 mM NaCl, 0.5 mM $CaCl_2$, 0.5 mM $MgCl_2$ and 10 mM HEPES) at pH 6.80, 7.40 or 8.00 three times, the intracellular pH was adjusted by using the same buffer at different pH in the presence of nigericin (1 μg/mL) and valinomycin (0.5 μg/mL). Confocal images were taken after 5 min.

Results and Discussion

Aza-BODIPY Dyes

Dye **1** has 2 tertiary amines and 2 phenols. The lone pair electrons of the N- and O- atoms cause the quench of fluorescence through PET and ICT processes. Methylation of the phenols, or the amines, or both produced **2**, **3** and **4**, respectively. So for **1**, the fluorescence can only be "turned on" when both the N- and O- are protonated. For **2** and **3**, protonation of the N- and O- respectively should activate the fluorescence. **4** as an "always on" control should not be affected by protonation. The resulting molecules also have different charges: **1** and **2** are neutral; **3** and **4** are positively charged. Methylation of the phenols increases the hydrophobicity of the dyes: the HPLC retention time for **1**, **2**, **3**, and **4** is 13.6, 19.8, 13.4, 19.6 min, respectively (protonated forms, see Supporting Information). These slight differences in structures induced significantly different intracellular fluorescence properties, as described below. Although the structures of control compounds **2** and **4** have been reported previously,[13, 21] their fluorescent properties in hydrophobic microenvironment and cytoplasm have not been studied.

Absorbance and Fluorescence Spectra

The dyes **1**-**4** showed similar UV-vis absorbance maximum around 696-704 nm when all the tertiary amine N- and phenol O- are protonated under acidic conditions (Figure 1A). The fluorescent emission maximum showed more difference: **4** has the lowest Em_{max} at 723 nm and **3** has the highest Em_{max} at 744 nm (Figure 1B). The near-infrared absorbance and fluorescence ensured minimal interference when imaging biological samples.

Fluorescence pH Titrations

Fluorescence pH titrations were performed in buffer-MeOH solution (1:1) at the dye concentration of 1 μM. All dyes showed very low fluorescence at physiological pH (~7.4) (Figure 1C), except for the "always-on" control **4**, whose fluorescence remained constant between pH 4.0-8.0. The fluorescence of **1**-**3** was activated as the pH decreased, corresponding to the protonation of the molecules and hence the suppression of the PET and/or ICT process. The fluorescence reached a plateau when all the species were protonated, where the fluorescence enhancements are over 30-fold based on the pH variation. The apparent pK_as of **1**-**3** are estimated to be 6.2, 6.6 and 6.2, respectively. These results indicate that the fluorescence of these dyes should respond to the pH in the acidic intracellular organelles.

Fluorescence Response to pH in micelles

It is documented that their apparent pK_as can shift significantly when fluorescent molecules are mixed with micelles, through both electrostatic and hydrophobic interactions; and the latter interaction is more dominant.[24-26] In many cases, neutral and anionic charged surfactants increase the pK_a, while cationic surfactants decrease the pK_a. The fluorescence response of dyes **1**-**4** (0.3 μM) to pH 7.4-10.2 in micelles were measured with commonly used surfactants SDS (anionic), CTAB (cationic), and Triton-X 100 (TX-100, neutral) in PBS (to mimic intracellular ionic strength). The 50 mM surfactant concentrations, which are much higher than their CMCs, were used so that micelle concentrations are similar under all conditions. Also, based on the surfactant aggregation numbers (60-140),[27] the concentrations of micelles are at least 2 orders of magnitude higher than those of the dyes. This ensures that there is an average of less than 1 dye per micelle, which should keep the interactions between dye molecules minimal.

As shown in Figure 2, the fluorescence of **1**-**3** is activated even at basic pH. For dye **1** (Figure 2A), the pK_a in SDS and TX-100 shifted well above physiological pH, while the pK_a in CTAB was ~6.8. The high fluorescence in CTAB is probably due to the increased quantum yield in more hydrophobic microenvironment after dye-CTAB charge neutralization, a result of less mobility hence less non-radiative decay. For dye **2** (Figure 2B), the high fluorescence at all pHs indicates that the pK_a in all 3 micelle solutions are above the pH range tested. Dye **3** showed similar pK_a shifts as dye **1**, but much lower activated fluorescence, possibly because it is positively charged and relatively more hydrophilic, thus weaker hydrophobic interactions with the surfactants. The activation of fluorescence at pH 7.40 can only happen when micelles form, i.e. no fluorescence at low surfactant concentration, as illustrated with dye **1** (see Supporting Information Figure S1). Additionally, no fluorescence was observed in MeOH solutions of the dyes **1**-**3** alone or dyes + surfactants, further proving the importance of hydrophobic interactions in fluorescence activation (data not shown). A detailed mechanism discussion about dye-micelle interaction can be found elsewhere[24] and will not be presented here. For dye **4** (Figure 2D), the fluorescence is constant under all conditions, since the micelles only help to disperse the dye molecules. Dye **4** in PBS (without surfactants) showed minimal fluorescence because of low solubility. It showed similar fluorescence in MeOH as in the micelle PBS solutions (data not shown). As expected, similar to solvation effects, the association of the dyes within different micelles resulted in different shifts in emission maximum (see Supporting Information Figure S2). In summary, the pK_as of dye **1**-**3** increase significantly in all micellar solutions. In other words, the fluorescence can be activated in micelles under neutral to basic pHs.

Fluorescence Response to pH in Liposomes

Although the cells lack micellar structures, they are rich in membrane structures, such as plasma membranes, endosome/lysosome membranes, and endoplasmic reticulum (ER), which are also hydrophobic in nature, but are much more complex than single component micelles. To test whether membrane structures can also “turn-on” the fluorescence, fluorescence response in liposomes at various pHs was measured. The liposomes are composed of lecithin-cholesterol (85:15 w/w), whose components are more related to cellular membranes and the bilayered structure can mimic the cellular membranes. The sizes of liposomes are very similar (120-130 nm, see Supporting Information Table S1) at all pH. As seen in Figure 3A, the fluorescence of **1**-**3** is activated at neutral pH, with pK_as well above physiological pH. The fluorescence activation of **3** is not as efficient as the other compounds of this series, similar to that seen in micelles. Again, no fluorescence was seen when mixing dye **1**-**3** with lecithin-cholesterol in MeOH, in which liposomes do not form (data not shown). For the “always-on” dye **4**, the fluorescence does not change much in response to pH. These results demonstrate that the fluorescence can be turned-on in liposomes at neutral to basic pH, through the pK_a shift in the bilayered structures.

Fluorescence Response to Ions and Biomolecules at Neutral pH

Because of the complexity of intracellular environment, the fluorescence responses of synthesized dyes to common ions and biomolecules at neutral pH (pH 7.40, PBS) were also measured. As shown in Figure 3B entries 2-20, at concentrations equal to or larger than their normal physiological concentrations, the ions and small biomolecules cannot “turn on” the fluorescence of the dyes. So this possibility of fluorescence activation can be excluded in the cellular experiments. The minimal fluorescence of dye **4** in the presence of ions and small biomolecules is mainly because of the lack of solubility. The interaction between **1** or **3** and DNA (2.5 mg/mL) resulted in a little fluorescence, while the more hydrophobic **2** or **4** did not show this effect (Figure 3B entry 21). When mixed with a model protein (BSA 25 mg/mL), **1** and **2** showed some fluorescence (Figure 3B entry 22), possibly through both

electrostatic and hydrophobic interactions with the protein. The higher fluorescence of more hydrophobic **2** implied the larger effect of the latter interaction. In comparison, the charged and relatively hydrophilic **3** did not show any fluorescence in the presence of BSA. For the "always on" control **4**, the protein helped its dispersion in solution and it showed quite high fluorescence, similar to what was seen with micelles and liposomes.

No-wash Live Cell Imaging

To visualize the intracellular activation of fluorescence of these dyes, MDA-MB-435 cells were incubated with the dyes (final concentration 0.1 μM) and live cells were imaged continuously for 30 min without washing the cells using confocal laser scanning microscope. As seen in Figure 4A-C, dyes **1**-**3** showed minimal background signals, because they are non-fluorescent under neutral pH. Dye **4** had some background fluorescence possibly because the serum proteins in the cell media helped solubilize the dye (Figure 4D). Similar to other small hydrophobic molecules, the uptakes of these dyes were quite fast. At 1 min, the cytoplasm membrane staining could be clearly seen for **1**, **2** and **4**, implying that the fluorescence was activated once the dyes were incorporated into the cell membranes.

The cytoplasm of cells stained with **1** was highly fluorescent after 30 min (Figure 4A 30 min), with cytoplasmic/extracellular fluorescent contrast ratio reaching ~10:1 within 10 min and staying constant (Figure 4E). At 30 min, the fluorescence at cellular membrane was not so obvious and was distributed throughout the cytoplasm, while the nucleus only showed very weak fluorescence. The spatial distribution of fluorescence clearly showed that the fluorescence of pH-sensitive dye **1** was "turned on" not only in acidic organelles, since these organelles normally have punctate vesicle-like structures, such as the commercial endosome/lysosome probe Lysotracker™ (Invitrogen, Carlsbad CA) has shown.[28-30] The brightest fluorescent area centers inside the cyto plasm and around the perinuclear region, where endoplasmic reticulum (ER) is located. Since the ER is rich in membrane structures, these observations agree well with the results obtained earlier (Figure 2 and 3). It should be noted that the distribution and intensity of fluorescence is determined by cellular uptake, dye molecule spatial distribution, and the extent of fluorescence activation. Similar fluorescence images were obtained with U-87 MG and HUVEC cells as well (data not shown). After incubation with **1** for 3 h, the cells were washed and incubated with fresh media. Images taken at later time points showed that the cytoplasmic fluorescence persisted even after 3 days (Figure 4F). The fluorescence contrast ratios at 3 h, 1, 2, and 3 days are 9.4, 4.5, 4.2, 4.5, respectively. The fluorescence was well retained considering the dilution of dyes resulting from cell proliferation. A possible reason is that the incorporation of the dye within cellular components slowed down the efflux (leakage) process significantly. No cell morphological changes were observed. The bright and long-lasting intracellular fluorescence of **1** makes it an excellent choice for live cell imaging and *in vivo* cell tracking.

After the cells were incubated with **2** for 30 min, the cytoplasm is also fluorescent, with cellular membrane still clearly stained (Figure 4B). The extracellular (or background) signal of **2** is more evident than that of **1** and **3**, which is probably caused by the interaction between **2** and serum protein (10% FBS in cell medium), as 2 also showed some fluorescence in the presence of BSA (Figure 3B entry 22). Within the cytoplasm, the fluorescent signals are not as uniform; the ER region seems the brightest. This may result from the relative hydrophobicity of **2** and thus its preferred accumulation in the more hydrophobic membrane structures. The fluorescent signal and contrast ratio of **3** is the lowest among all dyes (Figure 4C and 4E). Its charge and relative hydrophilicity may have impeded its cellular uptake. Also, the fluorescent activation of **3** in hydrophobic environment is the weakest, as seen in earlier experiments (Figure 2 and 3). For the "always on" dye **4**, the background (media) signal is the highest (Figure 4D); and its charge may

result in less efficient cellular uptake and dispersion within intracellular components. These are possible reasons for the low contrast ratio of **4**. Again, none of the pH-sensitive dyes showed staining pattern of acidic organelles, proving that pH is not the major factor of their fluorescent activation intracellularly.

Since we observed some fluorescence activation in the presence of BSA (Figure 3B entry 22), the same live cell imaging experiments were also performed after loading the dye in cell media without FBS. The results (Supporting Information Figure S3) showed very similar intracellular fluorescence distributions and signal contrast ratios for the all the dyes, indicating that the interaction between the dyes and extracellular FBS does not affect their intracellular fluorescence significantly.

Intracellular Fluorescence Distribution

To confirm the intracellular fluorescence distribution, the cellular components were separated by differential centrifugation (Figure 5A) after incubating the cells with the dyes **1**, **2**, or **4** for 2 h and the fluorescence of each fraction was measured (see Experimental Section). Because of its low intracellular fluorescence, this experiment was not carried out with dye **3**. As summarized in Figure 5B, fraction P, which contains the plasma membranes and fragments of ER, showed the highest fluorescence. Fractions M and R+C also showed some fluorescence, while fractions F and N only had minimal fluorescence. These results are consistent with our previous findings: the membrane structures showed high fluorescence, resulting from both preferred distribution and highest fluorescence activation. The fluorescence of fractions M and R+C could be from both proteins and the membranes of mitochondria, lysosomes and ribosomes. The minimal fluorescence in fraction N, similar to that in cellular imaging, showed the lack of dye distribution and/or activation in the nuclei.

Intracellular Fluorescence at Different pHs

We have shown that the fluorescence of **1** was "turned on" intracellularly as a result of pK_a shift when incorporated in membranes and proteins. Next, the fluorescence images of **1** were taken at different intracellular pHs. The cells were first incubated with the dye for 1 h; after removal of dye and washing with K^+-rich buffer at pH 6.80, 7.40 or 8.00, the intracellular pH was adjusted using the same buffer at respective pH in the presence of nigericin and valinomycin (see Experimental Section). Confocal images taken after 5 min are shown in Figure 6. The average intensities of cytoplasm fluorescence at pH 6.80, 7.40 and 8.00 were 649, 2190 and 843, respectively (see Supporting Information Figure S4). Most importantly, at pH 8.00, the fluorescence intensity was not quenched and not significantly different from that at more acidic pH 6.80. This further confirms that the fluorescence is "turned on" through protonation when incorporated in cellular components and the pK_a has shifted above physiological pH.

It can also be seen that under these conditions, the distribution of fluorescence has changed. As shown in the highlighted regions in Figure 6 (please bear in mind that not all the cells are on the same focal plane), the fluorescence showed many punctate vesicle-like structures, albeit evenly distributed fluorescence still can be seen. This is more evident at pH 6.80 and 8.00 than at physiological pH 7.40. This phenomenon, as well as the observation that the fluorescent intensity is much higher at pH 7.40, could be explained by two possible reasons. First, the degree of protonation of the dye is different at different pH, which affects its distribution. Second, the pH and experimental condition may change the conformation and assembly of intracellular proteins and membranes, which consequently altered their interaction with the dye and weakened the fluorescence activation. The pH of intracellular organelles may not reach equilibrium in a short time, hence stronger fluorescence is observed in vesicle-like structures.

Conclusion

We have synthesized and characterized three pH-sensitive NIR aza-BODIPY dyes. In bulk solution, these dyes are highly fluorescent only under acidic conditions, resulting from the suppression of PET and/or ICT process upon protonation. However, when they are incorporated in hydrophobic microenvironment (micelles, liposomes, hydrophobic pockets of proteins), they are highly fluorescent at neutral or even basic pH. pH titrations show that their apparent pK_a shift significantly towards more alkaline pH, in some cases even well above physiological pH.

The no-wash live cell imaging shows that their fluorescence is activated intracellularly, with minimal extracellular background. When these pH-sensitive dyes are uptaken by the cells, instead of staining only acidic organelles, they are fluorescent in the whole cytoplasm, indicating the fluorescence activation by intracellular components rather than pH. The fluorescence distribution shows that the fractions rich in membrane structures (plasma membrane and ER) have the highest fluorescence. The similar intracellular fluorescent intensities of dye **1** at pH 6.80 and 8.00 further confirmed that the intracellular fluorescence activation is not pH dependent.

Although these dyes are structurally very similar, the difference in charge and hydrophobicity result in significant differences in fluorescence intensity and distribution, most likely due to the difference in cellular uptake, intracellular distribution and fluorescence activation. Among the dyes, **1** shows the highest fluorescence contrast (~10) at a very low concentration (0.1 μM), and evenly stained cytoplasm. Moreover, its intracellular fluorescence can retain for several days, possibly because the incorporation into cellular components slows down the efflux process. These fluorescence properties of **1** make it an excellent choice for no-wash live cell imaging and *in vivo* cell tracking. These findings also imply that the intracellular fluorescent properties of pH-sensitive dyes should be carefully examined before used as pH indicators.

Supplementary Material

Refer to Web version on PubMed Central for supplementary material.

Acknowledgments

This work is supported by Intramural Research Program (IRP) of the National Institute of Biomedical Imaging and Bioengineering (NIBIB), National Institutes of Health (NIH). This work was performed while X-X Zhang held a National Research Council Research Associateship Award by NIBIB/NIST.

References

1. Gottlieb RA, Dosanjh A. Mutant cystic fibrosis transmembrane conductance regulator inhibits acidification and apoptosis in C127 cells: possible relevance to cystic fibrosis. Proc Nat Acad Sci USA. 1996; 93(8):3587–3591. [PubMed: 8622979]
2. Gottlieb RA, Nordberg J, Skowronski E, Babior BM. Apoptosis induced in Jurkat cells by several agents is preceded by intracellular acidification. Proc Nat Acad Sci USA. 1996; 93(2):654–658. [PubMed: 8570610]
3. Gottlieb RA, Giesing HA, Zhu JY, Engler RL, Babior BM. Cell acidification in apoptosis: granulocyte colony-stimulating factor delays programmed cell death in neutrophils by up-regulating the vacuolar H(+)-ATPase. Proc Nat Acad Sci USA. 1995; 92(13):5965–5968. [PubMed: 7541139]
4. Liang E, Liu P, Dinh S. Use of a pH-sensitive fluorescent probe for measuring intracellular pH of Caco-2 cells. Int J Pharm. 2007; 338(1–2):104–109. [PubMed: 17363203]

5. Walker NM, Simpson JE, Levitt RC, Boyle KT, Clarke LL. Talniflumate Increases Survival in a Cystic Fibrosis Mouse Model of Distal Intestinal Obstructive Syndrome. J Pharmacol Exp Ther. 2006; 317(1):275–283. [PubMed: 16354791]
6. Varadi A, Rutter GA. Ca2+-Induced Ca2+ Release in Pancreatic Islet β-Cells: Critical Evaluation of the Use of Endoplasmic Reticulum-Targeted "Cameleons". Endocrinology. 2004; 145(10):4540–4549. [PubMed: 15217981]
7. Simon S, Roy D, Schindler M. Intracellular pH and the control of multidrug resistance. Proc Nat Acad Sci USA. 1994; 91(3):1128–1132. [PubMed: 8302842]
8. Lakadamyali M, Rust MJ, Babcock HP, Zhuang X. Visualizing infection of individual influenza viruses. Proc Nat Acad Sci USA. 2003; 100(16):9280–9285. [PubMed: 12883000]
9. Izumi H, Torigoe T, Ishiguchi H, Uramoto H, Yoshida Y, Tanabe M, Ise T, Murakami T, Yoshida T, Nomoto M, Kohno K. Cellular pH regulators: potentially promising molecular targets for cancer chemotherapy. Cancer Treat Rev. 2003; 29(6):541–549. [PubMed: 14585264]
10. Davies TA, Fine RE, Johnson RJ, Levesque CA, Rathbun WH, Seetoo KF, Smith SJ, Strohmeier G, Volicer L, Delva L, Simons ER. Non-age Related Differences in Thrombin Responses by Platelets from Male Patients with Advanced Alzheimer's Disease. Biochem Biophys Res Commun. 1993; 194(1):537–543. [PubMed: 8333868]
11. Ohkuma S, Poole B. Fluorescence probe measurement of the intralysosomal pH in living cells and the perturbation of pH by various agents. Proc Nat Acad Sci USA. 1978; 75(7):3327–3331. [PubMed: 28524]
12. Han J, Burgess K. Fluorescent Indicators for Intracellular pH. Chem Rev. 2009; 110(5):2709–2728. [PubMed: 19831417]
13. Tasior M, Murtagh J, Frimannsson DO, McDonnell SO, O'Shea DF. Water-solubilised BF2-chelated tetraarylazadipyrromethenes. Org Biomol Chem. 2010; 8(3):522–525. [PubMed: 20090964]
14. Murtagh J, Frimannsson DO, O'Shea DF. Azide Conjugatable and pH Responsive Near-Infrared Fluorescent Imaging Probes. Org Lett. 2009; 11(23):5386–5389. [PubMed: 19883098]
15. McDonnell SO, Hall MJ, Allen LT, Byrne A, Gallagher WM, O'Shea DF. Supramolecular Photonic Therapeutic Agents. J Am Chem Soc. 2005; 127(47):16360–16361. [PubMed: 16305199]
16. Adarsh N, Avirah RR, Ramaiah D. Tuning Photosensitized Singlet Oxygen Generation Efficiency of Novel Aza-BODIPY Dyes. Org Lett. 2010; 12(24):5720–5723. [PubMed: 21090576]
17. Gorman A, Killoran J, O'Shea C, Kenna T, Gallagher WM, O'Shea DF. In Vitro Demonstration of the Heavy-Atom Effect for Photodynamic Therapy. J Am Chem Soc. 2004; 126(34):10619–10631. [PubMed: 15327320]
18. Coskun A, Yilmaz MD, Akkaya EU. Bis(2-pyridyl)-Substituted Boratriazaindacene as an NIR-Emitting Chemosensor for Hg(II). Org Lett. 2007; 9(4):607–609. [PubMed: 17256867]
19. Gawley RE, Mao H, Haque MM, Thorne JB, Pharr JS. Visible Fluorescence Chemosensor for Saxitoxin. J Org Chem. 2007; 72(6):2187–2191. [PubMed: 17298099]
20. Liu H, Mack J, Guo Q, Lu H, Kobayashi N, Shen Z. A selective colorimetric and fluorometric ammonium ion sensor based on the H-aggregation of an aza-BODIPY with fused pyrazine rings. Chem Commun. 2011; 47(44):12092–12094.
21. Hall MJ, McDonnell SO, Killoran J, O'Shea DF. A Modular Synthesis of Unsymmetrical Tetraarylazadipyrromethenes. J Org Chem. 2005; 70(14):5571–5578. [PubMed: 15989339]
22. Dopp E, von Recklinghausen U, Hartmann LM, Stueckradt I, Pollok I, Rabieh S, Hao L, Nussler A, Katier C, Hirner AV, Rettenmeier AW. Subcellular Distribution of Inorganic and Methylated Arsenic Compounds in Human Urothelial Cells and Human Hepatocytes. Drug Metab Dispos. 2008; 36(5):971–979. [PubMed: 18256204]
23. Thomas JA, Buchsbaum RN, Zimniak A, Racker E. Intracellular pH measurements in Ehrlich ascites tumor cells utilizing spectroscopic probes generated in situ. Biochemistry. 1979; 18(11):2210–2218. [PubMed: 36128]
24. Garcia MED, Sanz-Medel A. Dye-surfactant interactions: a review. Talanta. 1986; 33(3):255–264. [PubMed: 18964075]

25. Appell M, Bosma WB. Effect of surfactants on the spectrofluorimetric properties of zearalenone. J Luminescence. 2011; 131(11):2330–2334.

26. Freire S, Bordello J, Granadero D, Al-Soufi W, Novo M. Role of electrostatic and hydrophobic forces in the interaction of ionic dyes with charged micelles. Photochem Photobiol Sci. 2010; 9(5): 687–696. [PubMed: 20442928]

27. Kalyanasundaram, K. Photochemistry in Microheterogeneous Systems. Academic Press; New York: 1987.

28. Yahiro K, Satoh M, Nakano M, Hisatsune J, Isomoto H, Sap J, Suzuki H, Nomura F, Noda M, Moss J, Hirayama T. Low-density Lipoprotein Receptor-related Protein-1 (LRP1) Mediates Autophagy and Apoptosis Caused by Helicobacter pylori VacA. J Biol Chem. 2012; 287(37): 31104–31115. [PubMed: 22822085]

29. Hailey DW, Rambold AS, Satpute-Krishnan P, Mitra K, Sougrat R, Kim PK, Lippincott-Schwartz J. Mitochondria Supply Membranes for Autophagosome Biogenesis during Starvation. Cell. 2010; 141(4):656–667. [PubMed: 20478256]

30. Zhou R, Yazdi AS, Menu P, Tschopp J. A role for mitochondria in NLRP3 inflammasome activation. Nature. 2011; 469(7329):221–225. [PubMed: 21124315]

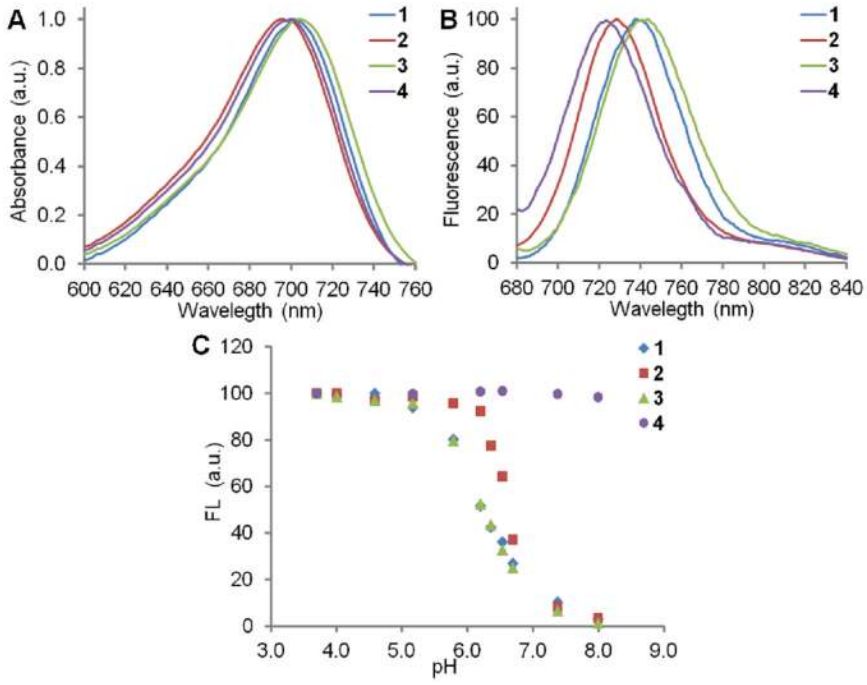

Figure 1.

A: Normalized UV-vis absorbance of **1**-**4** in 25 mM HCl MeOH-H_2O (1:1). B: Normalized fluorescence (Ex = 650 nm) of **1**-**4** in 25 mM HCl MeOH-H_2O (1:1). C: Fluorescence response of **1**-**4** (1 μM) in MeOH-Na_2HPO_4/citric acid buffer (1:1) at different pHs.

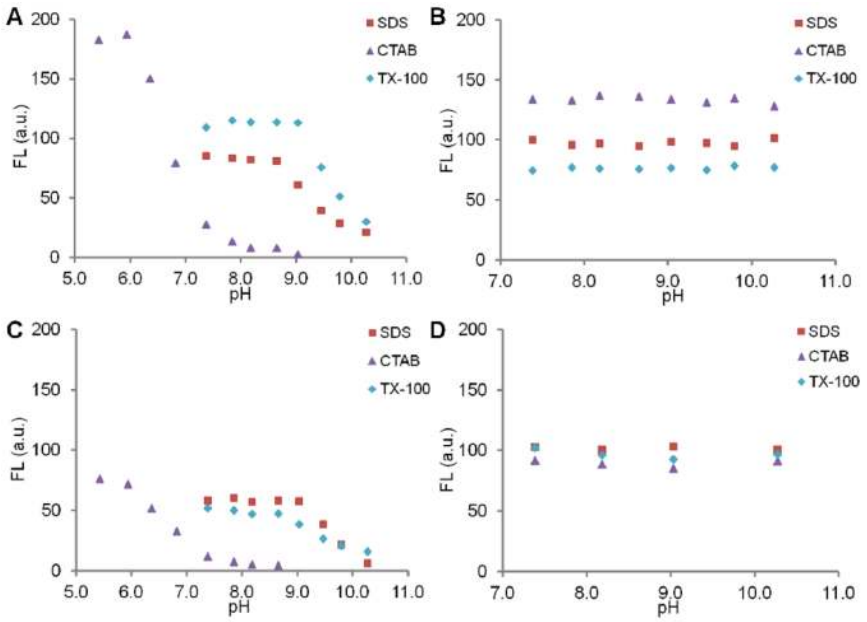

Figure 2.

Fluorescence response of **1**-**4** (A: **1**, B: **2**, C: **3**, D: **4**, 0.3 μM) in SDS, CTAB and TX-100 micelle solutions (50 mM in PBS) at different pHs. No fluorescence in the MeOH solutions of dye + surfactant except for **4** (data not shown). The fluorescence is normalized to FL = 100 under acidic conditions for each dye.

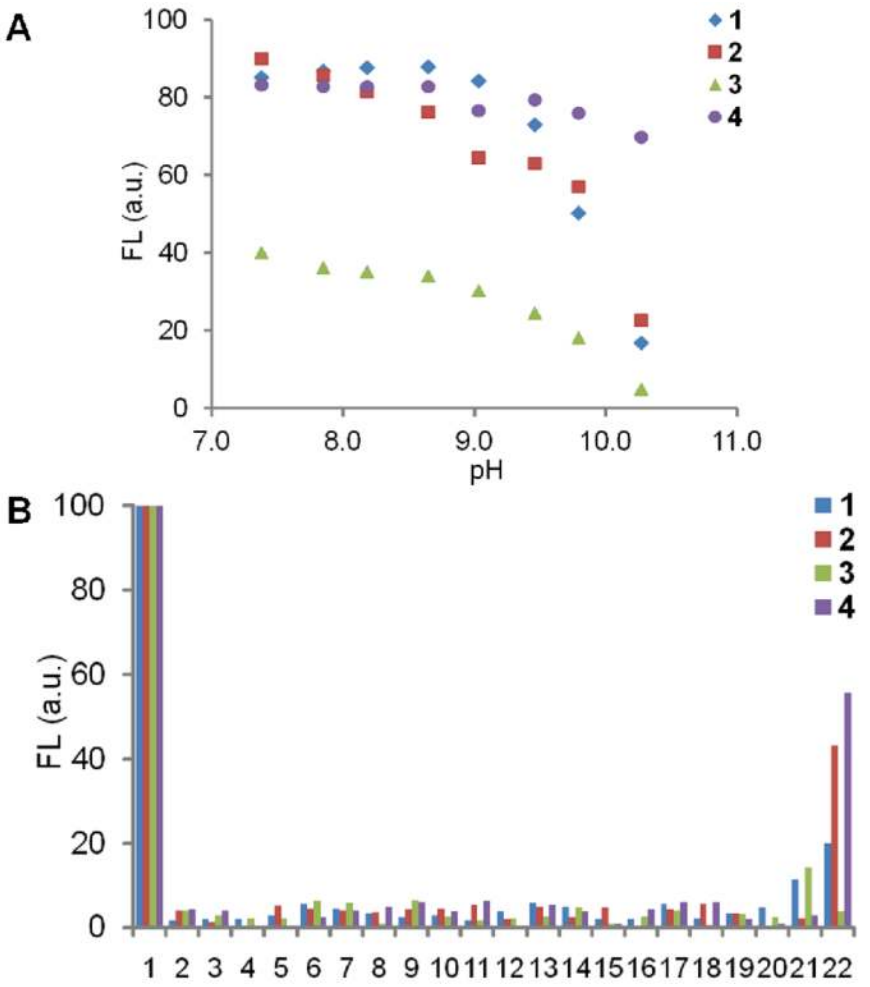

Figure 3.

A: Fluorescence response of **1**-**4** (0.3 μM) in 1 mg/mL lecithin-cholesterol (85/15 w/w) liposomal solutions at different pHs. No fluorescence in the MeOH solutions of dye + lecithin-cholesterol was seen except for **4** (data not shown) B: Fluorescence response of **1**-**4** (0.3 μM) in HEPES (10 mM, pH 7.40) to metal ions and biomolecules (5 mM unless otherwise specified). 1, dye only (protonated); 2, Na^+ (150 mM); 3, K^+ (150 mM); 4, Ca^{2+}; 5, Mg^{2+}; 6, Zn^{2+}; 7, Cu^{2+}; 8, cysteine; 9, glycine; 10, proline; 11, tyrosine (2.5 mM); 12, tryptophan; 13, glutamic acid; 14, histidine; 15, arginine; 16, lysine; 17, alanine; 18, dopamine; 19, glutathione; 20, vitamin C; 21, calf thymus DNA (2.5 mg/mL); 22, BSA (25 mg/mL). The fluorescence was normalized to FL = 100 under acidic conditions for each dye.

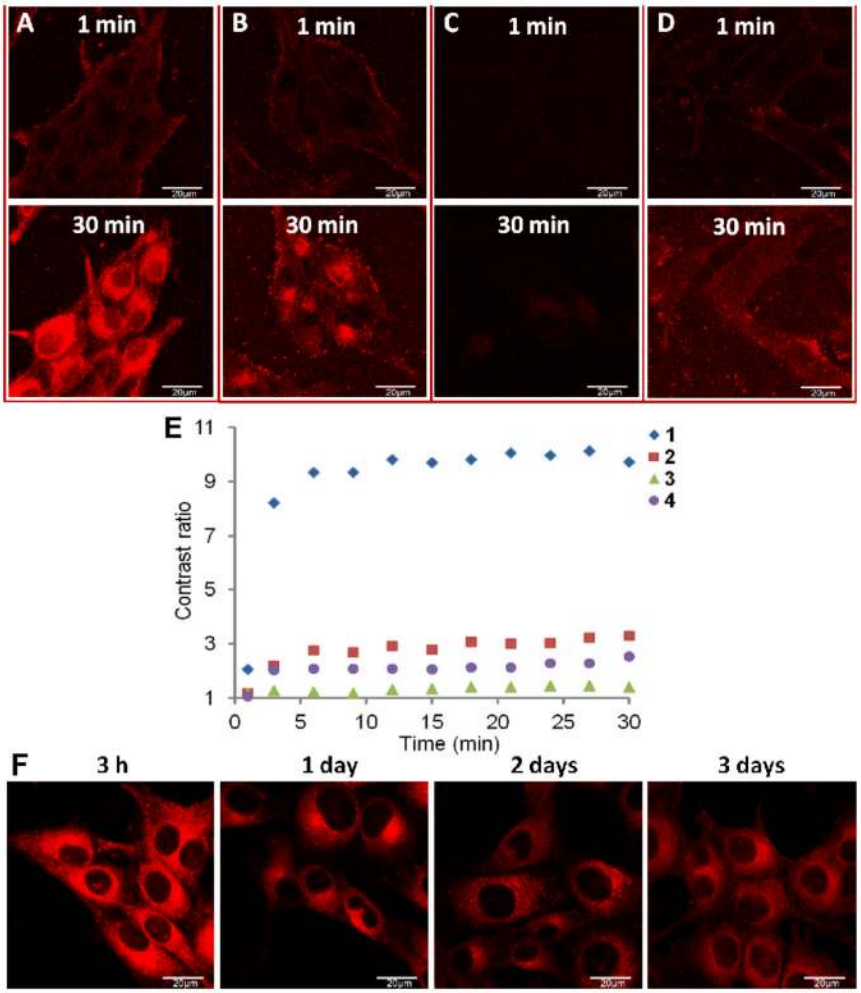

Figure 4.

A-D: Live cell imaging after adding respective dyes (A: **1**, B: **2**, C: **3**, D: **4**, final concentration: 0.1 μM) into MDA-MB-435 cells. Confocal fluorescent images taken at 1 min and 30 min after adding dyes and without washing the cells are shown. E: Cytoplasmic/extracellular fluorescent contrast ratios at different time points after adding **1**-**4**. F: live cell images of dye **1** labeled cells after 3 h, 1, 2, and 3 days. Cells were incubated with **1** for 3 h and then washed and kept under normal conditions. All images were taken under same microscopic settings and shown with same photographic settings (see Experimental Section).

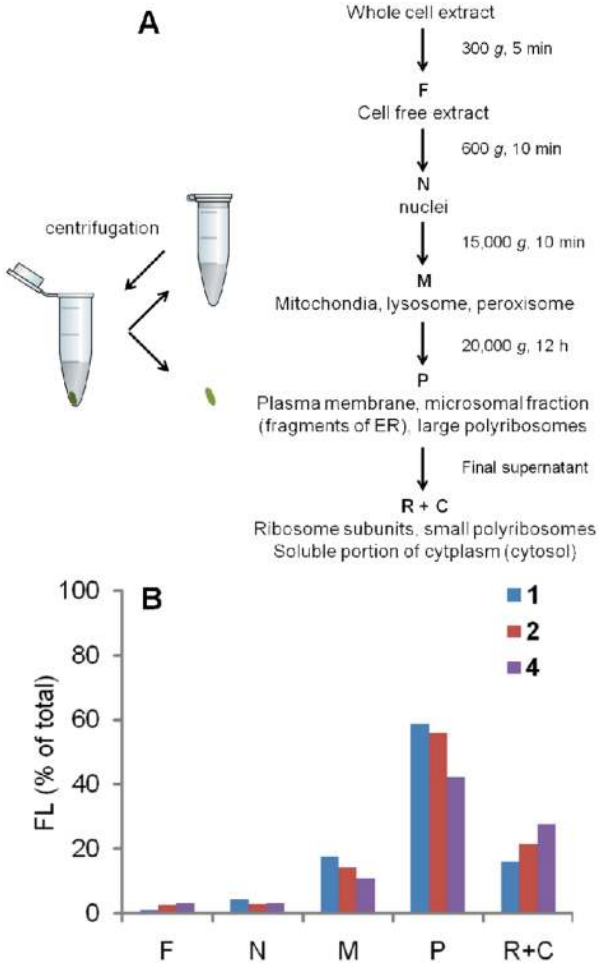

Figure 5.

Intracellular fluorescence distribution of **1**, **2**, and **4**. A: Method of separating cellular organelles using differential centrifugation. B: Comparison of fluorescence (% of total intracellular fluorescence for each dye) in different cellular fractions after incubation with the dyes for 2 h.

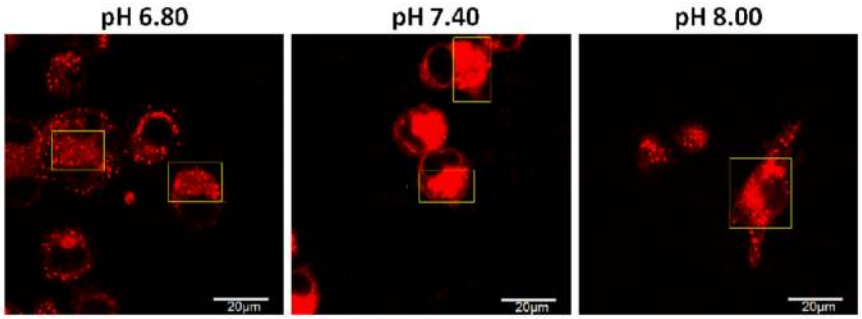

Figure 6.

Comparison of fluorescence at different intracellular pH. After incubation with **1** for 1 h, the intracellular pH of MDA-MB-435 cells was adjusted using K^+-rich buffer (130 mM K^+, 20 mM Na^+, 0.5 mM Ca^{2+}, 0.5 mM Mg^{2+} and 10 mM HEPES) in the presence of nigericin (1 μg/mL) and valinomycin (0.5 μg/mL). Live cell images were taken after 5 min.

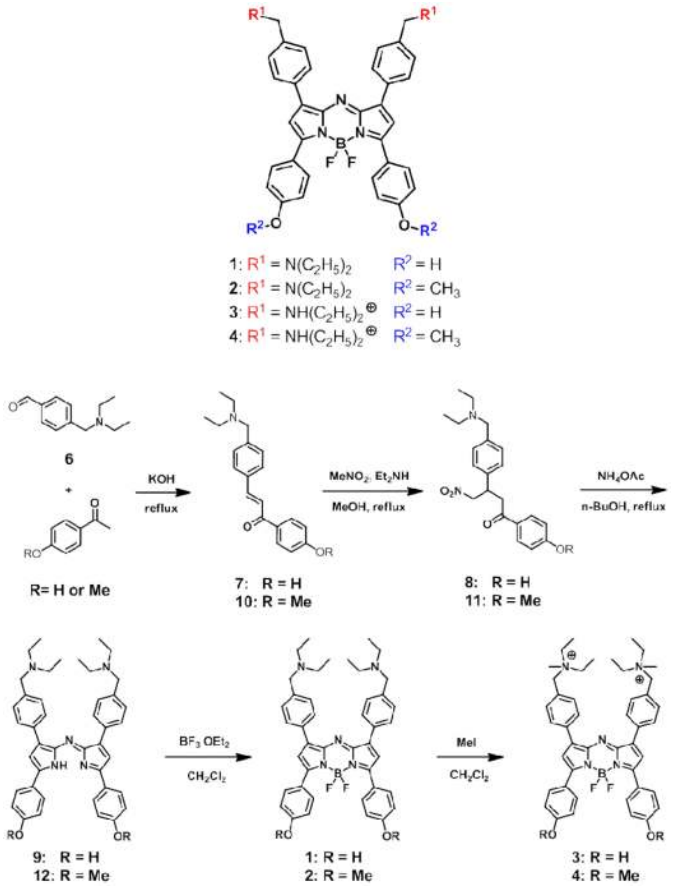

Scheme 1.
Ph-sensitive aza-BODIPY dyes and their synthetic route.